JOURNAL OF PROPULSION AND POWER
Vol. 18, No. 3, May–June 2002

Combustion of Liquefying Hybrid Propellants: Part 2, Stability of Liquid Films

M. A. Karabeyoglu* and B. J. Cantwell†
Stanford University, Stanford, California 94305

The stability of a liquid layer under strong blowing and subjected to large shear forces is investigated. This case is of practical importance for application to the regression rate estimation of liquefying hybrid rocket fuels such as solid cryogenic hybrids. An Orr–Sommerfeld equation for the linear stability of the liquid–gas interface is derived, and an exact solution is found for a linear base velocity profile. The exact solution for the liquid phase is coupled with the linearized gas-phase response with appropriate boundary conditions at the interface to give an eigenvalue problem for the linear stability of the layer. The results for liquid layer Reynolds numbers of practical interest (50–300) show the existence of a range of unstable wave numbers. It is observed that both the most amplified wave number and the maximum amplification increases with the liquid Reynolds number. It is also discovered that increasing surface tension and liquid viscosity have a stabilizing effect on the film. This prediction is supported by experimental results showing fast burning rates for low-viscosity fuels such as solid cryogenic pentane and noncryogenic wax. Finally, the stability theory is applied to the classical polymeric hybrid propellants that burn by forming a melt layer. Because the melt layers of these polymeric materials are highly viscous, they can not sustain thin film instabilities.

Nomenclature

A_n	=	power series solution coefficient
B	=	transform variable, $-ib/(\alpha Re)^{1/3}$
B_g	=	gas-phase blowing parameter
b	=	regression rate parameter
C_f, C_{f_0}	=	skin-friction coefficient with blowing and without blowing
c	=	amplification parameter, $c = \beta/\alpha$
c_n	=	exact solution coefficient
D	=	differential operator
d_p	=	port diameter
Fr	=	Froude number
$f_g(\zeta)$	=	viscous solution for the gas-phase Orr–Sommerfeld equation
G	=	port mass flux, $U_g^0 \rho_g$
g	=	body force per unit mass
h	=	melt layer thickness
I	=	gas-phase velocity profile integral [see Eq. (44d)]
i	=	unitary complex number
P	=	liquid-phase pressure
P_d	=	dynamic pressure in the port
$\tilde{P}_g$	=	nondimensional gas-phase normal stress perturbation
p	=	pressure perturbation in the liquid
Re	=	liquid layer Reynolds number
Re_g	=	gas-phase Reynolds number
$\dot{r}$	=	regression rate
$U_g(\zeta)$	=	mean velocity of the gas flow
U_g^0	=	gas velocity at the center of the port
U_l, U_l^0	=	mean axial velocity of the liquid at the interface with and without blowing
$U_0(y)$	=	mean axial velocity of the liquid
u	=	liquid velocity along the axis
V_l	=	mean normal velocity of the liquid
v	=	liquid velocity in the normal direction
We	=	Weber number
x	=	axial distance along the axis of the port
y	=	normal distance in the liquid
z	=	transform variable [see Eq. (31)]
α	=	nondimensional wave number
β	=	amplification parameter
Δ	=	gas-phase stress perturbation parameter [see Eq. (44c)]
δ	=	interface disturbance amplitude
δ_m	=	liquid layer momentum thickness
ζ	=	normal curvilinear coordinate in the gas phase
η	=	surface waveform
μ	=	viscosity
ρ	=	density
σ	=	surface tension
τ_g	=	mean shear stress exerted by the gas flow on the liquid–gas interface
$\tilde{\bar{\tau}}_g$	=	nondimensional gas-phase shear stress perturbation
$\varphi(x, y, t)$	=	liquid-phase stream function
$\phi(y)$	=	y component of $\varphi(x, y, t)$
$\psi(\zeta)$	=	inviscid solution for the gas-phase Orr–Sommerfeld equation

Subscripts

d	=	dimensional variable
g	=	gas-phase properties
l	=	liquid-phase properties

Superscripts

$\sim$	=	perturbation quantity
-	=	nondimensional quantity
$'$	=	transformed variable

Received 2 February 1999; revision received 8 January 2002; accepted for publication 10 January 2002.

*Research Associate, Department of Aeronautics and Astronautics. Member AIAA.
†Professor, Department of Aeronautics and Astronautics. Member AIAA.

Introduction

SOME hybrid rocket propellants, such as the solid cryogenic propellants, burn by forming a melt layer at the combustion surface. In Ref. 1, various effects of melt layer formation on the

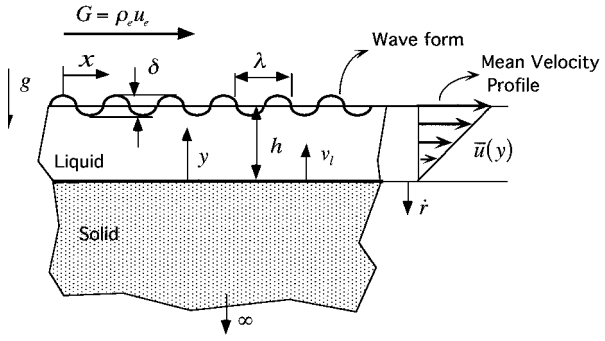

Fig. 1 Schematic of the stability model.

performance of the motor are discussed. Specifically, a theory that postulates the existence of entrainment from the liquid surface as a mass transfer mechanism, in addition to the vaporization, is developed. It is determined that the calculated burning rates are in good agreement with the experimentally observed values for cryogenic hybrid rockets utilizing frozen hydrocarbons as the solid propellant. An expression for the melt layer thickness is formulated, and it is shown that during typical operating conditions of a hybrid motor a melt layer with a reasonable thickness can be formed. The instability of the liquid film formed on the surface of a hybrid fuel grain is essential for the possibility of entrainment from the liquid interface. Although the stability of liquid layers were extensively studied in the past,[2–5] the behavior of films under strong blowing conditions and relatively high liquid Reynolds numbers, which are encountered in hybrids, has not been explored. In this paper, we will investigate the linear stability of a liquid layer with strong blowing under the effect of strong shear force generated by the gas flow in the port.

A schematic of the liquid layer stability model is shown in Fig. 1. In our investigations, we ignore the effect of density variations and all chemical reactions in the gas phase on the stability. In the calculations, we modify and adapt the linearized gas-phase equations derived by Benjamin[6] for the incompressible flow over a wavy wall. Because our predictions for the Reynolds numbers for the hybrid liquid films are typically on the order of a couple of hundreds, both the small Reynolds number and the high Reynolds number approximations[2,3] introduced in the literature as the solution techniques for the film stability equation are not satisfactory. For that reason, we develop new solution techniques for the liquid layer aspect of the problem.

The body force g is taken in the normal direction to make direct comparison with the previous stability work reported in the literature.[3] Note that, for a spin-stabilized rocket, the centrifugal acceleration will generate a body force in the normal direction acting outward as indicated in Fig. 1. The effect of axial acceleration of a missile on the stability is not addressed in this paper. Because the melt layer thicknesess are very small for typical hybrid fuels, it is fair to state that, for moderate accelerations, the effect of the axial body force on the stability is small compared to the dominant effect of the shear forces generated by the gas flow in the port.

Derivation of the Liquid-Phase Stability Equation

In this section the hydrodynamic stability equation for the liquid layer formed on the solid fuel grain is derived. For hybrid applications, the liquid layer Reynolds numbers defined with respect to the liquid layer thickness are estimated to be less than 300. Thus, the liquid flow in the layer can be assumed to be laminar in nature. In our analysis, we ignore the variations of the fluid properties across the thickness of the layer. We believe that the effect of these variations on the stability behavior of the film is small.

We start with the incompressible Navier–Stokes equations for a fluid with constant physical properties[2]:

$$\frac{\partial u}{\partial t} + u\frac{\partial u}{\partial x} + v\frac{\partial u}{\partial y} = \frac{\mu_l}{\rho_l}\nabla^2 u - \frac{1}{\rho_l}\frac{\partial P}{\partial x} \tag{1a}$$

$$\frac{\partial v}{\partial t} + u\frac{\partial v}{\partial x} + v\frac{\partial v}{\partial y} = \frac{\mu_l}{\rho_l}\nabla^2 v - \frac{1}{\rho_l}\frac{\partial P}{\partial y} \tag{1b}$$

$$\frac{\partial u}{\partial x} + \frac{\partial v}{\partial y} = 0 \tag{1c}$$

The film stability model for a hybrid motor must take into account the generation and injection of liquid at the solid interface and removal of the liquid at the gas interface. During the steady-state operation for which the film thickness is constant, the removal rate must be equal to the injection rate. In our study, we concentrate on this steady-state situation just described. Even in this simple state of operation, the liquid layer equations with respect to the rocket frame of reference does not possess a steady-state component. To simplify the analysis, the problem has to be formulated in a frame of reference that is fixed to the moving interfaces, which are translated at a constant speed with respect to the rocket frame. The new set of governing equations with respect to this moving reference frame can be obtained on the application of the following translational transformation on the Navier–Stokes equations:

$$x' = x, \qquad y' = y + \dot{r}t, \qquad u' = u$$

$$v' = v + \dot{r}, \qquad P' = P$$

It can be shown that the Navier–Stokes equations are invariant under this transformation, namely, the equations keep their forms with the new set of primed variables defined in the transformation equations. (For the sake of simplicity, from now on we drop the prime notation.) For that reason, Eqs. (1a–1c) also govern the dynamics of the fluid motion with respect to the moving reference of frame, and these equations will be used in the stability investigations.

In the moving reference of frame, there exists a steady component of the flowfield. It is reasonable to assume the following base flow, which is the steady part of the flowfield in the liquid layer:

$$v_0(x, y, t) = V_l, \qquad u_0(x, y, t) = U_0(y) \tag{2}$$

Here V_l is the mean velocity of the liquid in the film in the direction normal to the undisturbed liquid surface. This component of the velocity is assumed to be uniform in the whole domain. Moreover, the parallel component of the mean velocity is considered to be independent of the axial dimension. The substitution of the base flow expressions in the Navier–Stokes equations yields

$$V_l\frac{\mathrm{d}U_0}{\mathrm{d}y} = \frac{\mu_l}{\rho_l}\frac{\mathrm{d}^2U_0}{\mathrm{d}^2y} - \frac{1}{\rho_l}\frac{\partial P_0}{\partial x}, \qquad \frac{\partial P_0}{\partial y} = 0 \tag{3}$$

We further assume that the mean pressure is uniform in space, namely, P_0 is a function of time alone. This simplifies the description of the mean flow to the following ordinary differential equation (ODE) for the parallel velocity component:

$$\frac{\mu_l}{\rho_l}\frac{\mathrm{d}^2U_0}{\mathrm{d}^2y} - V_l\frac{\mathrm{d}U_0}{\mathrm{d}y} = 0 \tag{4}$$

This equation can easily be integrated to give

$$U_0(y) = (\tau_g/\rho_l V_l)\exp[-(V_l\rho_l/\mu_l)h]\{\exp[(V_l\rho_l/\mu_l)y] - 1\} \tag{5}$$

Note that the boundary conditions used are the no-slip requirement at the wall and the shear force balance at the gas–liquid interface:

$$U_0|_{y=0} = 0, \qquad \tau_g = C_f P_d = \mu_l\left.\frac{\mathrm{d}U_0}{\mathrm{d}y}\right|_{y=h} \tag{6}$$

Here τ_g is the mean shear stress exerted by the gas flow on the liquid surface, C_f is the skin-friction coefficient, and P_d is the dynamic pressure of the gas flow defined as $\rho_g U_g^{02}$.

Note that the mean y-component velocity of the liquid flow can be written in terms of the regression rate of the slab after a simple mass balance consideration. Namely, the mass balance on the control volume placed at the liquid–solid interface requires $V_l = \dot{r}\rho_s/\rho_l$. At

this point, it is useful to define a regression rate parameter (which is also a liquid-phase blowing parameter) b as

$$b \equiv V_l h \rho_l / \mu_l = (\rho_s / \rho_l)(h/\delta_m) \tag{7}$$

where the momentum thickness for the liquid layer is defined as $\delta_m = \mu_l / \rho_l \dot{r}$. For typical operating conditions of hybrids, the liquid blowing parameter falls in the range of 0.1–1.0. The velocity expression takes a more compact form when it is written in terms of b, namely,

$$U_0(y) = U_l^0 \{\exp[b(y/h)] - 1\}/be^b \tag{8}$$

where $U_l^0 = \tau_g h / \mu_l$.

In the limit of zero liquid blowing, $\dot{r} = 0$, the application of the L'Hospital's rule yields the following linear velocity profile of the standard Couette flow, as expected:

$$U_0(y) = U_l^0 y \big/ h = \tau_g y / \mu_l \tag{9}$$

According to Eq. (8), the liquid velocity at the surface is

$$U_0(h) \equiv U_l = U_l^0 [e^b - 1]/be^b \tag{10}$$

In Fig. 2, the plot of the velocity profiles according to Eqs. (8) and (9) are shown for a typical blowing parameter value of 0.4. It is apparent that the exact velocity profile is quite different from the simple Couette flow profile. However, it is observed that, for values of b smaller than 0.8, the exact solution is fairly close to a linear variation from the zero wall value to the maximum velocity predicted by Eq. (10). Note that the first-order effect of the injection is to reduce the surface velocity of the liquid. For that reason, the following corrected linear profile is a good approximation for small blowing parameters:

$$U_0(y) = U_l^0 [(e^b - 1)/be^b](y/h) \tag{11}$$

The corrected linear velocity profile given by Eq. (11) will be used in the linear stability investigations as an approximation for the base flow. This simplification is essential for the analytic development of an explicit stability expression for the film layer.

Now we perturb the liquid flowfield around the base flow presented in the preceding paragraphs. We separate the flow variables into their base flow components and perturbation components as

$$u = U_0(y) + \tilde{u}(x, y, t), \qquad v = V_l + \tilde{v}(x, y, t)$$

$$P = P_0(t) + \tilde{P}(x, y, t)$$

Next, we substitute these expressions in the Navier–Stokes equations. After collecting the terms to the first order and performing the simplifications on the base flow terms, we obtain the following linear equations:

$$\frac{\partial \tilde{u}}{\partial t} + U_0 \frac{\partial \tilde{u}}{\partial x} + \tilde{u} \frac{\mathrm{d}U_0}{\mathrm{d}y} + \frac{1}{\rho} \frac{\partial \tilde{P}}{\partial x} = \frac{\mu}{\rho} \nabla^2 \tilde{u} - V_l \frac{\partial \tilde{u}}{\partial y} \tag{12a}$$

$$\frac{\partial \tilde{v}}{\partial t} + U_0 \frac{\partial \tilde{v}}{\partial x} + \frac{1}{\rho} \frac{\partial \tilde{P}}{\partial y} = \frac{\mu}{\rho} \nabla^2 \tilde{v} - V_l \frac{\partial \tilde{v}}{\partial y} - g \tag{12b}$$

$$\frac{\partial \tilde{u}}{\partial x} + \frac{\partial \tilde{v}}{\partial y} = 0 \tag{12c}$$

The pressure terms can be canceled from the first two of these equations by cross differentiation and subtraction. In short notation, the resulting set of equations become

$$\tilde{u}_{ty} - \tilde{v}_{tx} + U_0' \tilde{u}_x + U_0 \tilde{u}_{xy} - U_0 \tilde{v}_{xx} + U_0' \tilde{v}_y + U_0'' \tilde{v} = (\mu_l/\rho_l)(\tilde{u}_{xxy} + \tilde{u}_{yyy} - \tilde{v}_{xxx} - \tilde{v}_{yyx}) - V_l(\tilde{u}_{yy} - \tilde{v}_{xy}) \tag{13a}$$

$$\tilde{v}_t + U_0 \tilde{v}_x + \tilde{P}_y/\rho_l = (\mu_l/\rho_l)(\tilde{v}_{xx} + \tilde{v}_{yy}) - V_l \tilde{v}_y - g \tag{13b}$$

$$\tilde{u}_x + \tilde{v}_y = 0 \tag{13c}$$

We investigate the stability of the harmonic surface waves. Therefore, we assume the following waveform for the liquid–gas interface[3]:

$$\eta_d(x, y, t) = \delta \exp[i(\alpha_d x - \beta_d t)] \tag{14}$$

Next, we define a stream function of the following form, which is consistent with the assumed surface wave,

$$\varphi(x, y, t) = \phi_d(y) \exp[i(\alpha_d x - \beta_d t)]$$

$$\tilde{u} = \varphi_y, \qquad \tilde{v} = -\varphi_x \tag{15}$$

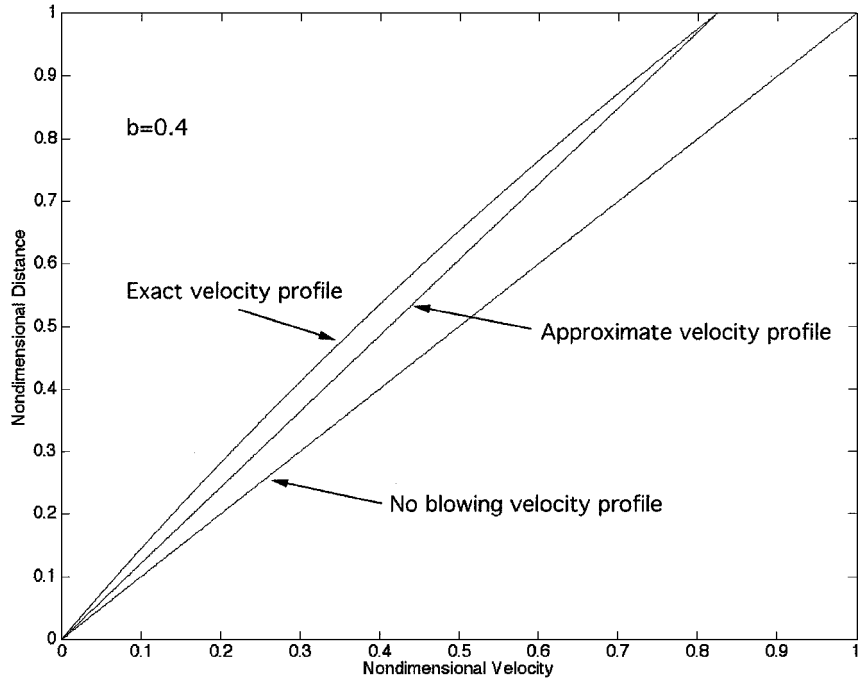

Fig. 2 Exact velocity profile for the regression rate parameter of $b = 0.4$; the linear approximation given by Eq. (11) and the velocity profile with no blowing are plotted.

Note that this definition of the stream function automatically satisfies the continuity equation and Eq. (13a) becomes a linear fourth-order ODE for the dependent variable ϕ_d:

$$(\alpha_d U_0 - \beta_d)\left(\phi_d'' - \alpha_d^2\phi_d\right) - \alpha_d U_0''\phi_d = -i(\mu_l/\rho_l)\left(\phi_d^{IV} - 2\alpha_d^2\phi_d'' + \alpha_d^4\phi_d\right) + iV_l\left(\phi_d''' - \alpha_d^2\phi_d'\right) \quad (16)$$

This is the Orr–Sommerfeld equation that governs the stability of a film layer with the steady-state injection of the fluid. For a pressure perturbation of the form $\tilde{P}(x, y, t) = p\exp[i(\alpha_d x - \beta_d t)]$, Eq. (13b) can be expressed as

$$p/\rho_l = \left[(\alpha_d U_0 - \beta_d)\phi_d' - U_0'\phi_d - (\mu_l/i\rho_l)\left(\phi_d''' - \alpha_d^2\phi_d'\right) + (V_l/i)\phi_d''\right](\eta_d/\alpha_d) \quad (17)$$

It is desirable to work with nondimensional quantities. For convenience, we introduce the following set of nondimensional variables:

$$\bar{t} = tU_l/h, \qquad \bar{x} = x/h, \qquad \bar{y} = y/h, \qquad \beta = \beta_d h/U_l$$

$$\alpha = \alpha_d h, \qquad \bar{U}_0 = U_0/U_l, \qquad \bar{v} = v/U_l, \qquad \eta = \eta_d/h$$

$$\bar{p} = p/\rho_l U_l, \qquad \phi = \phi_d/U_l h$$

The nondimensional version of Orr–Sommerfeld equation becomes

$$(\alpha\bar{U}_0 - \beta)(\phi'' - \alpha^2\phi) - \alpha\bar{U}_0''\phi = -(i/Re)[(\phi^{IV} - 2\alpha^2\phi'' + \alpha^4\phi) - b(\phi''' - \alpha^2\phi')] \quad (18)$$

where the liquid layer Reynolds number is defined as $Re = U_l h\rho_l/\mu_l$. The equation for the pressure perturbation can be written in terms of the nondimensional properties as

$$\bar{p} = \left[(\alpha\bar{U}_0 - \beta)\phi' - \bar{U}_0'\phi + (i/Re)(\phi''' - \alpha^2\phi') - ib\phi''\right](\eta/\alpha) \quad (19)$$

We use the approximate mean velocity expression given by Eq. (11), which simplifies to $\bar{U}_0 = \bar{y}$ in nondimensional form. On substitution of this linear velocity profile and some minor rearrangements, the Orr–Sommerfeld equation can be written in the following form:

$$\phi^{IV} - 2\alpha^2\phi'' + \alpha^4\phi - b(\phi''' - \alpha^2\phi') = i\alpha Re(\bar{y} - c)(\phi'' - \alpha^2\phi) \quad (20)$$

Here, c is defined as β/α for convenience. Note that this is a fourth-order linear equation with variable coefficients. In the next section we discuss the appropriate boundary conditions for the film stability problem.

Boundary Conditions

The first two of the boundary conditions can be obtained from the velocity requirements at the solid–liquid interface. The physical statement of the requirements are 1) the parallel component of the velocity at solid wall must be zero due to the no-slip condition and 2) the regression rate of the slab is steady. These conditions can be formulated as

$$\tilde{u}(0) = 0, \qquad \tilde{v}(0) = 0$$

These can be written in terms of the stream function formulation as

$$\phi(0) = 0, \qquad \phi'(0) = 0 \quad (21)$$

Another requirement that needs to be satisfied by the solution is the kinematic boundary condition at the liquid–gas interface. In the linear form this can be written as[3]

$$\bar{v}(1) = \frac{\mathrm{D}\eta}{\mathrm{D}\bar{t}} = \eta_{\bar{t}} + \eta_{\bar{x}}$$

In terms of the stream function the kinematic condition simplifies to

$$\phi(1) = 1 - c \quad (22)$$

There are two other constraints that limit the possibility of solutions, that come from the dynamic conditions at the liquid–gas interface. These are the shear and the normal force balances at the liquid surface. The shear force balance in the linear form requires

$$\bar{\tilde{\tau}}_g = \left(\mu_l/\rho_l U_l^2\right)(\tilde{u}_y + \tilde{v}_x)$$

In this relation, $\bar{\tilde{\tau}}_g$ is the nondimensional gas-phase shear stress perturbation on the liquid interface. Note that the gas shear perturbation should be determined by solving the gas-phase perturbation equations, which will be discussed later. For the present purposes, we consider $\bar{\tilde{\tau}}_g$ as a known input for the liquid layer stability problem. The definition of the stream function can be used to convert this equation into the stream function format as

$$\bar{\tilde{\tau}}_g/\eta = -(1/Re)[\phi''(1) + \alpha^2\phi(1)] \quad (23)$$

Finally, the normal force balance at the surface requires

$$-\bar{p} + (2/Re)\bar{v}_{\bar{y}} = \eta_{\bar{x}\bar{x}}/We + (\bar{\tilde{P}}_g - \eta/Fr)$$

Here $\bar{\tilde{P}}_g$ is the nondimensional gas-phase pressure perturbation on the liquid surface and

$$We = \rho_p U_l^2/\sigma h, \qquad Fr = U_l^2/gh \quad (24)$$

After converting this equation into the stream function format and coupling with the other boundary conditions, one obtains the following expression:

$$(1 - c)\phi'(1) - \phi(1) - (1/i\alpha Re)[\phi'''(1) - b\phi''(1) - 3\alpha^2\phi'(1)] = \left(\alpha^2/We + 1/Fr - \bar{\tilde{P}}_g/\eta\right)[\phi(1)/(1 - c)] \quad (25)$$

Equations (21–23), and (25) set five conditions on the fourth-order differential equation (20). Thus, this is an overposed boundary-value problem. The correct approach is to consider the Orr–Sommerfeld equation with those five conditions as an eigenvalue problem, the eigenvalue being the amplification parameter c. The direct numerical solution of this eigenvalue problem is computationally expensive because it requires many iterations (each iteration a finite difference solution itself) for every selection of the parameters such as the Reynolds number, Froude number, or the Weber number that might effect the stability of the layer. For that reason, it is desirable to develop analytical solutions. We obtain solutions for the stability problem by using two independent techniques. We first develop a power series solution that can only be applied to films with Reynolds numbers less than unity. For the power series solution, we modified Craik's technique,[3] which was originally applied to a simpler case of a layer with no blowing. Because, in hybrid applications, the film layer Reynolds numbers can be significantly larger than unity, we also formulated an exact solution for the liquid stability problem just defined. In the next section we discuss the development of the two distinct solutions.

Development of Solutions

Power Series Solution

Following Craik,[3] we assume a regular power series solution for the Orr–Sommerfeld equation (20) of the form

$$\phi(y) = \sum_{n=0}^{N} A_n \bar{y}^n \quad (26)$$

Next, this power series is substituted in the Orr–Sommerfeld equation to obtain the recurrence relations for the coefficients of the power series. The form of the recurrence relations implies that if the

following order of magnitude relations are valid, the power series converges rapidly:

$$\alpha^2 \ll 1, \qquad |-i\alpha Re| < \mathcal{O}(1), \qquad |-ic\alpha Re + 2\alpha^2| < \mathcal{O}(1)$$

$$|-ic\alpha Re + \alpha^2| < \mathcal{O}(1), \qquad b < \mathcal{O}(1)$$

We truncate the series at $n = 6$ under the assumption that the convergence rate is reasonably fast. The first seven coefficients of the series, which are of our concern, are calculated with the use of the recurrence relations. Eventually, the stream function ϕ can be expressed, to the first order, in terms of four unknown coefficients A_0, A_1, A_2, and A_3:

$$\phi(\bar{y}) = A_0 + A_1\bar{y} + A_2[\bar{y}^2 + (q/12)\bar{y}^4 - (p/60)\bar{y}^5] + A_3[\bar{y}^3 + (b/4)\bar{y}^4 + (q/20)\bar{y}^5 - (p/60)\bar{y}^6] \tag{27}$$

This approximate general expression can now be used to solve the eigenvalue problem specified by the boundary conditions. First, it is clear that the zero velocity conditions at the solid surface requires

$$A_0 = A_1 = 0 \tag{28}$$

The remaining boundary conditions set a new eigenvalue problem with reduced dimensions that can be solved to yield the following condition on the eigenvalue c (to the first order) for the existence of a solution:

$$\frac{\alpha^2}{We} + \frac{1}{Fr} - \frac{\bar{\bar{P}}_g}{\eta} + \frac{3i\bar{\tau}_g/\eta}{2\alpha} = (1-c)\left[\frac{3}{2}(1-c) - 1 + \frac{(3 + 3b + 6\alpha^2)}{i\alpha Re}\right] \tag{29}$$

This is the quadratic stability relation of the liquid film layer. For a selection of physical film parameters and gas-flow conditions, the sign of the imaginary part of the eigenvalue c determines the stability of the layer. The stability behavior of the layer according to this relation will be discussed later in this paper.

Exact Solution

The assumptions required for the convergence of the power series solution limit the range of applicability of the solution to Reynolds numbers and regression rate parameters less than one. However, the liquid layers formed on the walls of the hybrid fuel grain possess Reynolds numbers up to several hundred, due to the large shear forces exerted by the strong gas flow. In this range of moderate Reynolds numbers, the applicability of the high Reynolds number expansion solutions is also highly questionable. For that reason, we developed an exact solution for the eigenvalue problem stated. In this section we present the outline of our derivation.

It is convenient to restate the Orr–Sommerfeld equation in the operator format,

$$(\mathrm{D}^4 - b\,\mathrm{D}^3 - 2\alpha^2\,\mathrm{D}^2 + b\alpha^2\,\mathrm{D} + \alpha^4)\phi = [i\alpha Re(\bar{y} - c)](\mathrm{D}^2 - \alpha^2)\phi \tag{30}$$

where the differential operator is defined as $\mathrm{D} \equiv \mathrm{d}/\mathrm{d}\bar{y}$.

The critical step in the derivation is the factorization of the operator on the left-hand side of the equation as

$$(\mathrm{D}^2 - b\,\mathrm{D} - \alpha^2)(\mathrm{D}^2 - \alpha^2)\phi = [i\alpha Re(\bar{y} - c)](\mathrm{D}^2 - \alpha^2)\phi \tag{31}$$

After the factorization, this fourth-order equation can be separated into two second-order equations that can be expressed in the standard ODE notation as

$$\theta'' - b\theta' - [\alpha^2 + i\alpha Re(\bar{y} - c)]\theta = 0 \tag{32a}$$

$$\phi'' - \alpha^2\phi = \theta \tag{32b}$$

The first of these is a homogeneous linear equation with variable coefficients, whereas the second one is an inhomogeneous equation with constant coefficients. Our solution strategy is to first solve Eq. (32a) and use the result to determine the particular solution of the second equation.

We start the solution procedure of Eq. (32a) with the application of the following transformation

$$z = -\frac{\alpha^2 + i\alpha Re(\bar{y} - c)}{(\alpha Re)^{\frac{2}{3}}} \tag{33}$$

In terms of the transformed variable, the equation becomes

$$\frac{\mathrm{d}^2\theta}{\mathrm{d}z^2} + B\frac{\mathrm{d}\theta}{\mathrm{d}z} - z\theta = 0 \tag{34}$$

where $B = -ib/(\alpha Re)^{1/3}$.

Equation (34) takes a simpler form in its reduced form, $\theta = UV$. Here, the variable V is given by $V = \exp[-(B/2)z]$, and U is the solution of the following ODE[7]

$$\frac{\mathrm{d}^2U}{\mathrm{d}z^2} - z + \frac{B^2}{4}\frac{\mathrm{d}U}{\mathrm{d}z} = 0 \tag{35}$$

The ODE for U can further be simplified after the transformation $\xi = z + B^2/4$:

$$\frac{\mathrm{d}^2U}{\mathrm{d}\xi^2} - \xi\frac{\mathrm{d}U}{\mathrm{d}\xi} = 0 \tag{36}$$

This equation is commonly known as the Airy equation, and the solution can be readily written in terms of the Airy functions Ai and Bi (Ref. 7):

$$U(\xi) = c_1 Ai(\xi) + c_2 Bi(\xi) \tag{37}$$

Now, we transform back to the original nondimensional physical variables to obtain the solution

$$\theta(\bar{y}) = c_1 \exp[-(B/2)z(\bar{y})]Ai[z(\bar{y}) + B^2/4] + c_2 \exp[-(B/2)z(\bar{y})]Bi[z(\bar{y}) + B^2/4] \tag{38}$$

Note that z is a linear function of $\bar{y}$ by Eq. (33).

We are now in a position to solve Eq. (32b), which becomes

$$\frac{\mathrm{d}^2\phi}{\mathrm{d}\bar{y}^2} - \alpha^2\phi = c_1 \exp\left[-\left(\frac{B}{2}\right)z(\bar{y})\right]Ai\left[z(\bar{y}) + \frac{B^2}{4}\right] + c_2 \exp\left[-\left(\frac{B}{2}\right)z(\bar{y})\right]Bi\left[z(\bar{y}) + \frac{B^2}{4}\right] \tag{39}$$

The homogeneous solution of this equation is quite simple

$$\phi_h(\bar{y}) = c_1 e^{\alpha\bar{y}} + c_2 e^{-\alpha\bar{y}} \tag{40}$$

The particular solution can be obtained with use of the technique of variation of parameters. After some algebraic manipulations the total solution can be written as

$$\phi(\bar{y}) = \sum_{n=1}^{4} c_n\phi_n(\bar{y}) \tag{41}$$

where the four independent particular solutions of the Orr–Sommerfeld equation are

$$\phi_1 = e^{\alpha\bar{y}} \tag{42a}$$

$$\phi_2 = e^{-\alpha\bar{y}} \tag{42b}$$

$$\phi_3(\bar{y}) = \frac{1}{\alpha}\int_{\bar{y}_0}^{\bar{y}} \sinh[\alpha(\bar{y} - \hat{y})] \times \exp\left[-\left(\frac{B}{2}\right)z(\hat{y})\right]Ai\left[z(\hat{y}) + \frac{B^2}{4}\right]\mathrm{d}\hat{y} \tag{42c}$$

$$\phi_4(\bar{y}) = \frac{1}{\alpha}\int_{\bar{y}_0}^{\bar{y}} \sinh[\alpha(\bar{y}-\hat{y})] \times \exp\left[-\left(\frac{B}{2}\right)z(\hat{y})\right] Bi\left[z(\hat{y}) + \frac{B^2}{4}\right] \mathrm{d}\hat{y} \tag{42d}$$

In this format, the boundary conditions can be written explicitly as

$$\sum_{n=1}^{4} c_n \phi_n(0) = 0 \tag{43a}$$

$$\sum_{n=1}^{4} c_n \phi_n'(0) = 0 \tag{43b}$$

$$\sum_{n=1}^{4} c_n \left[\phi_n'(1) - \alpha^2 \phi_n(1)\right] = Re\frac{\bar{\bar{\tau}}_g}{\eta} \tag{43c}$$

$$\sum_{n=1}^{4} c_n \left\{\phi_n''(1) - b\phi_n''(1) - 3\alpha^2\phi_n'(1) + (i\alpha Re)[(c-1)\phi_n'(1) + \phi_n(1)]\right\} = i\alpha Re\left(\frac{\alpha^2}{We} + \frac{1}{Fr} - \frac{\bar{\bar{P}}_g}{\eta}\right) \tag{43d}$$

$$\sum_{n=1}^{4} c_n \phi_n(1) = c - 1 \tag{43e}$$

These boundary conditions with the analytical expressions for the independent solutions can now be used to solve the eigenvalue problem for the eigenvalue c. Note that the selection of $\bar{y}_0 = 0$ significantly simplifies the solution because the first two of the boundary conditions require $c_1 = c_2 = 0$ and drop out of the system. In this case, the system is reduced to three equations for three unknowns, c_3, c_4, and c. Note that even the reduced system involves difficult integrals and that it is nonlinear in c. Thus, the solution requires numerical integration and some iterative procedure on c. To perform the calculations, we developed a MATHEMATICA program that automates the solution procedure and iteratively solves the eigenvalue c, for any given selection of parameters. The time required for the solution at a specified point of the parameter space is less than a second with a modern desktop computer. Thus, the analytic solution developed for the film stability problem is apparently very efficient in terms of the computation time over the numerical simulation of the Orr–Somerfeld equation or the Navier–Stokes equations.

Gas Phase

The linear stability problem discussed in the preceding section requires the gas-phase response as the input. In this section we will describe the gas-phase perturbation treatment that was first developed by Benjamin[6] and later adapted to the thin-film stability problem by Craik.[3] Benjamin investigated the flowfield generated by a shearing gas flow on a wavy surface and presented explicit formulas for the shear and normal stresses disturbances induced by the shear flow on the surface. The following fundamental simplifications were introduced in the treatment:

1) Primary gas flow is parallel and in the direction of the surface waves.

2) In the case of a turbulent gas flow, the interactions with the turbulence and the wave motion are neglected. In other words, the mean velocity distribution for the turbulent case is disturbed by the waves in the same fashion as the velocity distribution in an equivalent laminar flow.

3) The complete solution for the Orr–Sommerfeld equation derived for the gas phase is expressed as a sum of the inviscid solution $\psi(\zeta)$ and a viscous solution confined to a small thickness next to the surface $f_g(\zeta)$, where ζ is the curvilinear coordinate that is perpendicular to the wavy surface. The viscous solution, which rapidly diminishes as one moves away from the surface, is required to satisfy the wall boundary conditions imposed on the fourth-order Orr–Sommerfeld equation. The region where $f_g(\zeta)$ is significant compared to the inviscid solution is called the wall friction layer, not to be confused with the viscous sublayer of a turbulent boundary layer.

The explicit solution for the shear stress and pressure perturbations presented by Benjamin[6] is revised and reformulated by Craik[3] in the context of the liquid layer stability problem formulated in the preceding section. We have discovered that the simplifying assumption, $\Delta \ll 1$, that was used by both Benjamin[6] and Craik,[3] significantly restricts the applicability of the gas-phase stress perturbation expressions given in Refs. 3 and 6. This assumption on Δ is particularly invalid for hybrid rocket applications, typically characterized by high gas velocities and small disturbance wavelengths. We followed Benjamin's[6] original derivation to refine the set of gas-phase stress perturbation formulas by relaxing the restricting assumption on Δ. We found that the nondimensional normal and the tangential stress perturbations $\bar{\bar{P}}_g$ and $\bar{\bar{\tau}}_g$, which are valid for any value of Δ, can be approximated by the following equations:

$$\frac{\bar{\bar{P}}_g}{\eta} = \frac{(\alpha/Re)}{1 + 1.288\exp(i\pi/6)\Delta}\left[\frac{I}{C_f} - 2i\right] \tag{44a}$$

$$\frac{\bar{\bar{\tau}}_g}{\eta} = 1.373\left(\frac{\mu_l}{\mu_g}\right)^{\frac{2}{3}}\frac{\rho_g}{\rho_l}\frac{I}{C_f}\frac{\exp(i\pi/3)\alpha^3(\alpha Re)^{-\frac{4}{3}}}{[1 + 1.288\exp(i\pi/6)\Delta]^2} \tag{44b}$$

$$\Delta = \frac{I}{C_f}\left(\frac{\mu_g}{\mu_l}\right)^{\frac{4}{3}}\left(\frac{\rho_l}{\rho_g}\right)^{\frac{2}{3}}(\alpha Re)^{-\frac{2}{3}}\alpha^2 \tag{44c}$$

$$I = \int_0^{\infty}\left(\frac{U_g}{U_g^0}\right)^2 \exp(-\alpha\zeta)\,\mathrm{d}(\alpha\zeta) \tag{44d}$$

Here, U_g is the mean boundary-layer velocity profile of the gas flow, U_g^0 is the gas velocity at the center of the port, and μ_g and ρ_g are the average viscosity and the density of the gas in the port, respectively. The real parts of stress parameters correspond to the components of stress that are in phase with the wave displacement, whereas the imaginary parts of the stress parameters represent the stress components, which are in phase with the wave slope.

Apart from the three general simplifications discussed in the preceding paragraph, the following specific assumptions restrict the applicability of Eqs. (44a–44d):

1) Both the dimensional wave velocity and the velocity of the liquid at the liquid–gas interface need to be small compared to the gas velocity in the center of the fuel port:

$$\beta_d/\alpha_d = cU_l \ll U_g^0, \qquad U_l \ll U_g^0 \tag{45}$$

Under these assumptions the liquid–gas interface can be treated as a rigid surface. For hybrid applications, both of these assumptions are easily satisfied.

2) The wavelength of the surface disturbance must be small compared to the port diameter:

$$\alpha d_p/h = kd_p \geq \mathcal{O}(1) \tag{46}$$

For the film thicknesses and mass fluxes typically encountered in hybrid rockets, this is a good approximation.

3) The wavelength of the surface disturbance needs to be small compared to the thickness of the wall friction layer. This condition can be expressed for the turbulent boundary layer of a hybrid rocket as

$$kx < 0.172B_g^{-0.34}Re_g^{0.9} \tag{47}$$

Here, $Re_g = Gx/\mu_g$ is the gas-phase Reynolds number, $k = \alpha/h$ is the dimensional wave number, x is the distance along the axis

of the port, B_g is the blowing parameter, and the port mass flux is defined as $G = U_g^0 \rho_g$. The blocking factor of the following form as suggested in Ref. 8 is used in the preceding inequality:

$$C_f / C_{f0} = B_g^{-0.68} \tag{48}$$

Also note that the blowing skin-friction coefficient is calculated from the following turbulent boundary-layer relation commonly used in hybrid rocket applications:

$$C_{f0} = 0.0296 Re_g^{-\frac{1}{5}} \tag{49}$$

4) The linear region of the velocity profile, viscous sublayer in the case of turbulent wall flows must cover the thickness of the wall friction layer. For the turbulent boundary layer of a hybrid rocket, this assumption implies the following condition:

$$kx > 1.720\,10^{-4} B_g^{-0.34} Re_g^{0.9} \tag{50}$$

The last two assumptions are fundamental to Benjamin's[6] treatment, and they are essential in obtaining an analytical expression for the rapidly decaying viscous component of the solution. Equations (44a–44d) for the gas-phase stress perturbations are derived for an incompressible gas flow with no blowing allowed. For that reason, note that the applicability of these relations to the hybrid boundary layer with combustion and strong blowing is a rough approximation.

5) The effect of blowing is assumed to be limited to the primary gas flow, that is, C_f. The influence of blowing on the flow perturbations in the gas phase is ignored.

6) The effect of chemical reactions and gas property variations across the boundary layer and along the axis of the rocket are ignored. We use average values for the gas-phase properties such as μ_g and ρ_g. For typical hybrid rocket conditions, the flame zone in which the majority of the chemical reactions and the heat release takes place is relatively remote from the surface. Thus, the wall friction layer and the flame zone do not overlap. We believe that this minimizes the coupling between the flow induced by the surface disturbances and chemical reactions.

For the sake of simplicity, the following form of the gas-phase velocity profile will be used in evaluating the integral I:

$$\frac{U_g(\zeta)}{U_g^0} = \left(\frac{2\zeta h}{d_p}\right)^{\frac{1}{7}}, \quad \text{for} \quad \zeta < d_p/2h \tag{51a}$$

$$\frac{U_g(\zeta)}{U_g^0} = \left(2 - \frac{2\zeta h}{d_p}\right)^{\frac{1}{7}}, \quad \text{for} \quad d_p/2h < \zeta < d_p/h \tag{51b}$$

Note that for hybrid rocket applications, the boundaries of the integral in Eq. (44d) need to be from 0 to d_p/h.

Finally, it can be shown that with use of the shear balance at the liquid–gas interface, the liquid layer Reynolds number can be written in terms of the gas-flow parameters and the properties of the liquid:

$$Re = Re_g^2 C_f (\rho_l/\rho_g)(\mu_g/\mu_l)^2 (h/x)^2 [(e^b - 1)/be^b] \tag{52}$$

Discussion of Results for Stability

In this section we present the results for the liquid layer stability problem that are obtained with the application of the solution techniques discussed in the preceding section. For all of the calculations that will be conducted in this paper, the following geometrical and gas-phase properties will be used, $d_p = 2$ cm, $x = 14$ cm, $\mu_g = 6.5\,10^{-6}$ Pa-s, and $\rho_g = 8$ kg/m^3. Liquid properties for various materials are listed in Table 1 (see Refs. 9 and 10). The solid densities of all of the cryogenic propellants are assumed to be equal to the density of solid pentane, 850 kg/m^3. The solid density of the wax is taken to be 930 kg/m^3. The gas-phase blowing parameter B_g, used in the calculations for all of the fuels, is seven.

It is important to demonstrate the validity of the gas-phase assumptions listed in the preceding section for a typical set of operating conditions, $G = 100$ kg/m^{2}s, $\dot{r} = 1$ mm/s, and $h = 0.3$ mm. For pentane as the working liquid, the ratio of the liquid interface velocity to the gas velocity in the center of the port is estimated to be 0.0359. This indicates that the conditions imposed by Eq. (45) are satisfied and that the first assumption is a valid one. For the selected operating point, the conditions on assumptions 2, 3, and 4 can be reduced to $k \geq 0.0714$ cm^{-1} and 0.339 cm$^{-1} < k < 3390$ cm^{-1}. All of these inequalities are satisfied over the range of wave numbers where the positive amplification takes place, (see Figs. 4–7). It can be shown that, for a wide range of operating conditions typically encountered in hybrids and over the wave numbers for which most of the positive amplification occurs, all conditions are satisfied and the use of the gas-phase equations (44a–44d) is acceptable.

First, we compare the result of the exact solution with the power series solution for verification purposes. Figure 3 shows the amplification rate (imaginary part of $c\alpha Re$) as a function of the wave number for the power series solution and also for the exact solution. Figure 3 is for a water film with a relatively low liquid Reynolds number of 5 and at a regression rate parameter b of 0.2. (For a given Reynolds number the corresponding Weber number can be calculated with use of the simple relation $We = (\mu_l/\rho_l h^3 \sigma) Re^2$.) The body force is assumed to be zero, and the film thickness is 0.3 mm. As can be deduced from Fig. 3, the exact solution is in good agreement with the power series predictions for the small Reynolds number used in the calculation, within the range of small wave numbers. As expected, the error associated with the power series solution increases rapidly with increasing nondimensional wave number.

One of the most interesting results of this linear theory is that even at very small film thicknesses there exists a finite range of amplified wave numbers, namely, the layer is unstable over a finite range of wave numbers. Instabilities of that type were first discovered for thin water films in a wind tunnel by Craik,[3] and they are called the slow waves. These are generated by the interaction of the gas-phase shear stresses acting on the liquid surface with the slope of the liquid layer surface. Figure 4 shows a typical form of the dimensional amplification rate of the interface disturbance, $-\mathrm{Im}(\beta_d)$, as a function of the dimensional wave number k calculated with use of the linear stability theory outlined in this paper. Note that the dimensional amplification rate can be expressed in terms of the nondimensional amplification rate as

$$-\mathrm{Im}(\beta_d) = -\mathrm{Im}(c\alpha Re)\left(\mu_l / h^2 \rho_l\right)$$

For this calculation, the liquid is water, liquid Reynolds number is 50, film thickness is 0.3 mm, regression rate is zero, and the Froude number corresponding to the body force of 9.81 m/s^2 is 9.458. As indicated in Fig. 4, there is a positive amplification domain that lies between two cutoff wave numbers. The amplification takes a maximum value at a wave number between these two cutoff wave numbers. This is the most amplified wave number, and the corresponding wavelength is expected to be the observed size of the disturbance in the actual flow system. As the body force diminishes, the first cutoff point moves toward zero.

Intuitively, the most important parameter that links the linear stability results to the entrainment rate of the liquid from the surface is the amplification rate of the disturbances. Figure 5 shows the effect of the liquid Reynolds number on the amplification curves. This plot is for a 0.3-mm-thick pentane film. The liquid Reynolds number is adjusted by changing the port mass flux from 42.7 kg/m$^2 \cdot$ s to 92.2 kg/m$^2 \cdot$ s. The regression rate parameter is 0.55, and the body force is assumed to be zero. Note that as the liquid layer Reynolds number (which is directly proportional to the gas-stream dynamic pressure) increases, the amplification rate increases. The Reynolds number also increases the most amplified wave number, meaning that at higher gas flow velocities the expected wavelengths of the instabilities are smaller. This latter result is in good agreement with the experimental findings for the scale of waves formed on the surface of a thin film.[11]

The effect of the liquid injection on the film stability is shown in Fig. 6. The amplification rate as a function of the wave number for three values of regression rate parameter b is calculated with use of

Table 1 Material properties of the liquids used in the calculations[9] [a]

Liquid	Pentane C_5H_{12}	HFI	Acetone C_3H_6O	Isopropanol C_3H_8O	Wax	Water H_2O
Molecular weight, g/mol	72.15	69.11	58.08	60.10	432.8	18
Surface tension, mN/m	14.3	15.6	19.2	16.4	7.1	72
Viscosity, mPa s	0.463	2.5	0.51	5.0	0.65	1.0
Density liquid phase, kg/m^3	688.4	785.0	835.2	808.9	654.4	1000
Melting temperature, K	143.3	181	178.45	183.3	339.6	273
Boiling temperature, K	309.6	350	329.44	355.4	727.4	373

[a] For liquids other than water all properties but the surface tension are evaluated at a mean temperature between the melting and vaporization temperatures. Surface tension is evaluated at the boiling temperature. Wax properties are estimated in Ref. 10. Water properties are at ambient conditions.

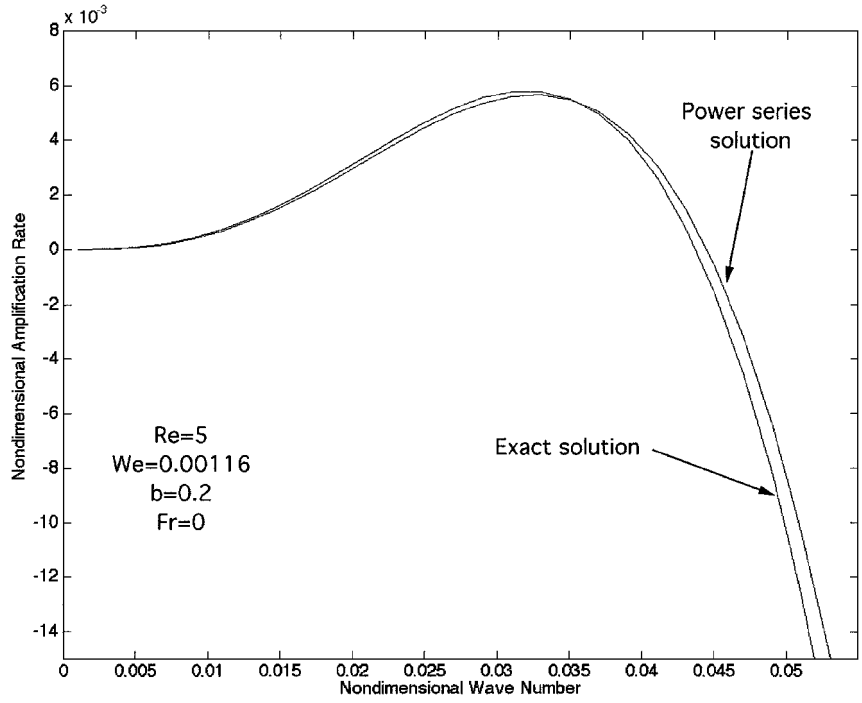

Fig. 3 Nondimensional amplification rate (i.e., imaginary part of αcRe) of a surface disturbance vs the nondimensional wave number α, calculated with the power series method and the exact solution method; this case is for a water film with a thickness of 0.3 mm, a liquid Reynolds number of 5, and a regression rate parameter of 0.2. (Body force is taken to be zero.)

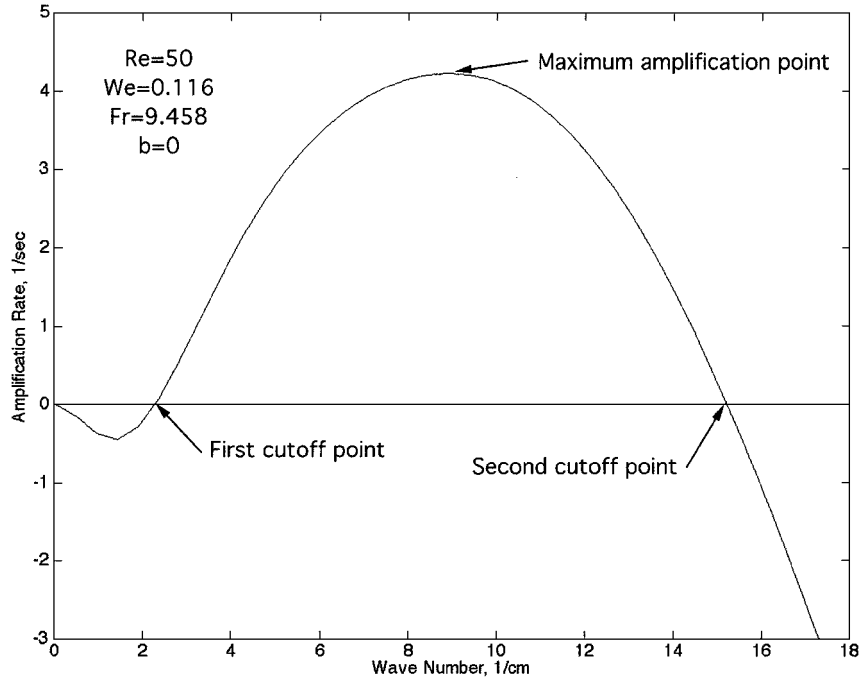

Fig. 4 Amplification rate of a surface disturbance vs the wave number; water film with a thickness of 0.3 mm and film Reynolds number of 50, Froude number is 9.458, and the regression rate parameter is zero.

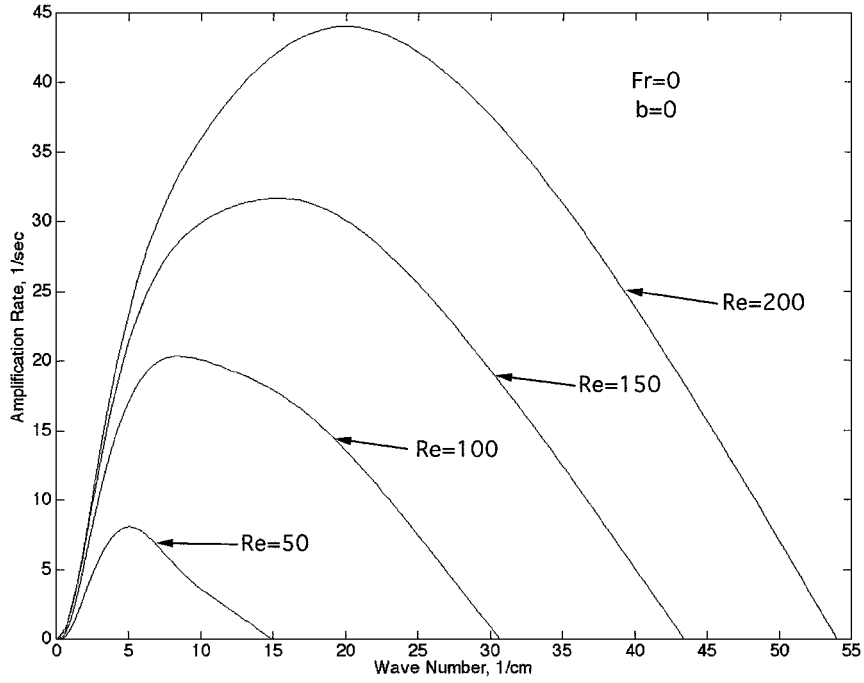

Fig. 5 Amplification rate of a surface disturbance vs the wave number for various film Reynolds numbers; pentane film with a thickness of 0.3 mm, Reynolds number is altered by changing the gas mass flux in the port. (Body force and the regression rate is taken to be zero for this calculation.)

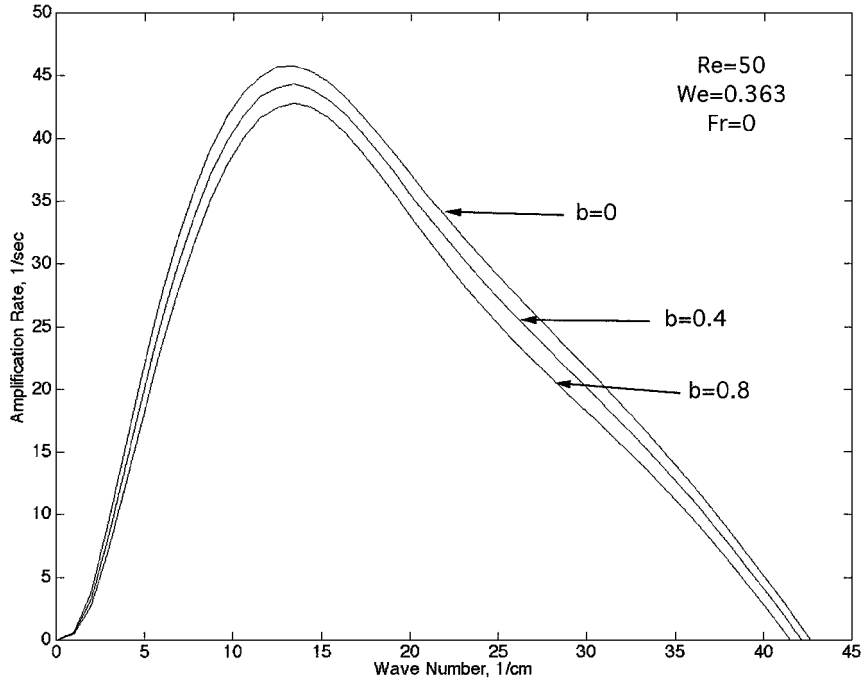

Fig. 6 Effect of regression rate on the stability of the film; pentane film with a thickness of 0.15 mm and a liquid Reynolds number of 50. (Body force is taken to be zero.)

the exact solution. This case is for a 0.15-mm pentane film with a liquid Reynolds number of 50 and a Froude number of zero. Figure 6 shows that the normal liquid injection has a slight stabilizing effect on the film. This conclusion is also confirmed by the power series solution. For a situation for which the mass flux is kept constant rather than the liquid Reynolds number, the effect of the regression rate parameter will be more dominant. This is because, according to Eq. (52), an increase in the regression rate parameter decreases the liquid Reynolds number for a given port mass flux value.

Another very important result that came out of the stability investigation is that both the surface tension and also the viscosity of the liquid have a stabilizing effect on the liquid film. It turns out that this feature of the thin-film instabilities plays a major role in determining which propellant is likely to sustain instabilities and potentially entrain droplets into the gas stream. To demonstrate the effect of material properties on the stability, the amplification curves for various liquids at a fixed film thickness of 0.15 mm are shown in Fig. 7. For all of the liquids, the regression rate is 1 mm/s and the port mass flux is 80 $kg/m^2 \cdot s$. Note that liquids with higher viscosities such as isopropanol and HFI are more stable than the liquids with small viscosity values. The stability curve for one grade paraffin wax, which is solid under ambient conditions, is included in Fig. 7.

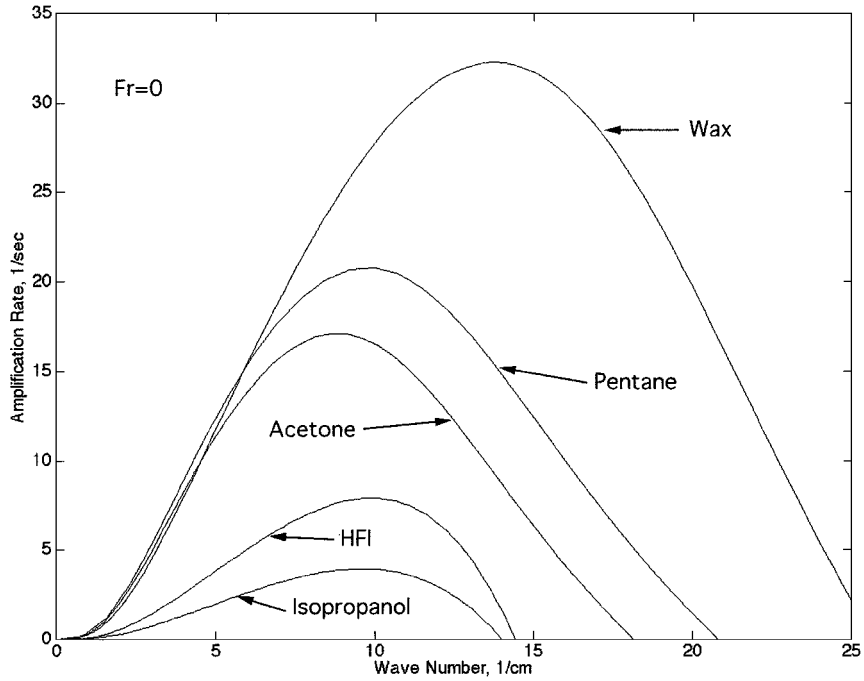

Fig. 7 Amplification curves for various liquids for a port gas mass flux of 80 kg/m^2 · s and a regression rate of 1 mm/s, film thickness of 0.15 mm used. (Body force is assumed to be zero.)

It is predicted by the theory that this particular grade of wax would form an unstable melt layer and possibly entrain liquid droplets into the gas stream. In support of this prediction, lab scale motor tests recently conducted at Stanford University using a similar grade wax resulted in very high regression rates. In fact, the regression rates for wax is determined to be on the same order of the burning rates observed for solid cryogenic pentane.[1]

As a final note, the linear stability theory developed in this paper can also be applied to classical hybrid propellants that form a liquid layer on their burning surfaces. One such propellant is high-density polyethylene (HDPE) polymer, which has been tested extensively as a hybrid fuel. In Ref. 10 it is shown that the melt layer of HDPE is four orders of magnitude more viscous than pentane. The linear theory suggests that the melt layers of these highly viscous polymeric fuels will be extremely stable at the port mass flux levels typically encountered in hybrid motors.

In practice, the linear instability of the liquid film is a necessary, but not a sufficient, condition for the onset of entrainment. Moreover, linear stability investigation can not be directly used for calculating the level of entrainment. The rigorous treatment of the entrainment problem requires a fully nonlinear investigation. In this study, we avoid this difficulty by assuming that the scaling of the amplification rate predicted by the linear theory gives a direct measure for the scaling of entrainment.

Conclusions

In this paper we discussed the linear stability of a film layer with blowing. It is shown that the layer can be unstable over a wide range of parameters. The maximum amplification and also the most amplified wave number both increase with increasing dynamic pressure (or mass flux) in the port for a given liquid at a constant film thickness. It is also shown that blowing has a small stabilizing influence on the film. Furthermore, the material properties of the liquid have an important role in the stability behavior of the liquid layer. Specifically, we have shown that increasing surface tension and liquid viscosity stabilizes the film. This observation is confirmed by motor tests performed with several solid cryogenic fuels and non-cryogenic wax. The linear theory is also applied to classical hybrid rocket fuels that burn by forming a melt layer. It has been shown that because the melt layers of these materials are very viscous, they cannot sustain the thin-film instabilities. Finally, for typical hybrid operating conditions, the effect of body forces on the stability of the film is negligible compared to the effect of the strong shear force generated by the gas flow in the port.

Acknowledgments

This work was partially supported by the NASA Ames Research Center and the Joint Institute for Aeronautics and Astronautics under Grants NCC2-55 and NCC2-1172. Additional funds were provided by Stanford University.

References

[1] Karabeyoglu, M. A., Altman, D., and Cantwell, B. J., "Combustion of Liquefying Hybrid Propellants: Part 1, General Theory," *Journal of Propulsion and Power* (submitted for publication).

[2] Schlichting, H., *Boundary Layer Theory*, McGraw–Hill, New York, 1955, pp 430–445.

[3] Craik, A. D. D., "Wind Generated Waves in Thin Liquid Films," *Journal of Fluid Mechanics*, Vol. 26, Pt. 2, 1966, pp. 369–392.

[4] Chang, I.-D., and Russel, P. E., "Stability of a Liquid Layer Adjacent to a High-Speed Gas Stream," *Physics of Fluids*, Vol. 8, No. 6, 1965, pp 1018–1026.

[5] Nayfeh, A. H., and Saric, W. S., "Non-Linear Kelvin-Helmholtz Instability," *Journal of Fluid Mechanics*, Vol. 46, Pt. 2, 1971, pp. 209–231.

[6] Benjamin, T. B., "Shearing Flow over a Wavy Boundary," *Journal of Fluid Mechanics*, Vol. 6, 1959, pp. 161–205.

[7] Gungor, F., "Diferansiyel Denklemler," Istanbul Teknik Universitesi, Istanbul, Turkey, 1995.

[8] Altman, D., and Humble, R., "Hybrid Rocket Propulsion Systems," *Space Propulsion Analysis and Design*, McGraw–Hill, New York, 1995, p. 382.

[9] Dauber, T. E., and Danner, R. T., *Physical and Thermodynamic Properties of Pure Chemicals, Data Compilation*, Taylor and Francis, Washington, DC, 1997.

[10] Karabeyoglu, M. A., "Transient Combustion in Hybrid Rockets," Ph.D. Dissertation, Dept. of Aeronautics and Astronautics, Stanford Univ., Stanford, CA, Aug. 1998.

[11] Gater, R. A., and L'Ecuyer, M. R., "A Fundamental Investigation of the Phenomena that Characterize Liquid Film Cooling," *International Journal of Heat and Mass Transfer*, Vol. 13, No. 3, 1970, pp. 1925–1939.